

Communication

A Comparison of the Performance of Two Kinds of Waterborne Coatings on Bamboo and Bamboo Scrimber

Jianfeng Xu ^{1,2,3,†}, Ru Liu ^{1,†} , Huagui Wu ¹, Hongyun Qiu ¹, Yanglun Yu ^{1,*}, Ling Long ^{1,2,*} and Yonghao Ni ³

¹ Research Institute of Wood Industry, Chinese Academy of Forestry, Haidian, Beijing 100091, China; xjf821211@163.com (J.X.); liuru@criwi.org.cn (R.L.); caf506peper@163.com (H.W.); qiuqiuiuu1307@163.com (H.Q.)

² Research Institute of Forestry New Technology, Chinese Academy of Forestry, Haidian, Beijing 100091, China

³ Department of Chemical Engineering, University of New Brunswick, Fredericton NB E3B 5A3, Canada; yonghao@unb.ca

* Correspondence: yuyanglun@caf.ac.cn (Y.Y.); longling@caf.ac.cn (L.L.); Tel.: +86-10-62889481 (Y.Y.); +86-10-62889425 (L.L.)

† These authors contributed equally to this work.

Received: 20 December 2018; Accepted: 27 February 2019; Published: 1 March 2019



Abstract: For this paper, two kinds of waterborne coatings, polyurethane acrylate (PUA) and epoxy resin, were synthesized and then coated onto neat bamboo and bamboo scrimber (BS), respectively. The coating performance of the samples was investigated. The results showed that, for the two kinds of coatings, there was a chemical reaction occurring between both coatings and the substrates. The permeability with respect to bamboo was higher than that of BS, while that of the epoxy resin coating was better than PUA. However, the PUA film was smoother than epoxy resin. The epoxy resin coating on bamboo had the best adhesion, which was at a 1 level. The abrasion values of the four samples varied in the same substrate. A higher hardness of the coating film was obtained when coated with PUA. In general, the coating performance of bamboo scrimber was poorer than that of bamboo, either coated with PUA or epoxy resin. The epoxy resin had a better coating performance than PUA.

Keywords: bamboo scrimber; coating performance; waterborne coating; polyurethane acrylate; epoxy resin

1. Introduction

Bamboo scrimber (BS) is a novel bamboo-based composite made from bamboo bundles compressed and bonded in the parallel direction. It has gradually become one of the main commercial products in the bamboo industry. During the forming processes of BS, there are many physical and chemical changes to bamboo cells, such as compressing, bonding, and densifying [1–5]. Compared with other bamboo composites, bamboo scrimber has comparatively higher raw material utilization rate because the bamboo bark has not been removed [6–10]. Therefore, bamboo scrimber has a desirable texture, high hardness, and longitudinal strength properties [11–14]. However, a dense structure and fewer hydrophilic groups are predicted because the parenchyma and bamboo fiber are compressed and filled with adhesive.

Recently, coating processes carried out on materials have received more and more attention because of their good protective and beautifying effects for various substrates [15–19]. With the development of greater environmental protection awareness, waterborne coatings play an important

role in coatings [20]. However, few studies focus on the coating techniques and processes of waterborne coating materials. A whole coating process includes facts such as substrate wetting, leveling, infiltrating, and drying into the film, so the hydrophilicity and porosity of the substrate have a great impact on the coating process and coating performance [21]. Thus, there is a large demand for research on the coating performance of bamboo scrimber, whose hydrophilicity and porosity differ greatly from those of wood.

For this paper, bamboo and bamboo scrimber were coated with polyurethane acrylate (PUA) and epoxy resin coating. The coating performance of those materials was investigated, aiming to compare different types of waterborne coatings for bamboo and bamboo scrimber.

2. Materials and Methods

2.1. Materials

Maso bamboo (*Phyllostachys pubescens*), age 3–4 years, was taken from the Jian'ou Forest Reserve, Fujian Province of China. The reagents for the waterborne coatings are listed in Table 1.

Table 1. Reagents for waterborne coatings.

| Reagent | Type | Abbreviation | Manufacturer |
|--|------------------------|--------------|--------------|
| Ammonium persulfate | Initiator | APS | 1 |
| Acrylic acid | Monomer | AA | 1 |
| Styrene | Monomer | ST | 1 |
| Ethyl acrylate | Monomer | EA | 1 |
| Hydroxyethyl acrylate | Monomer | HEA | 1 |
| Toluene-2,4-diisocyanate | Monomer | TDI | 1 |
| Polyethylene glycol (M_n : 400) | Monomer | PEG-400 | 1 |
| Dibutyltin dilaurate | Catalyzer | DBTD | 1 |
| γ -aminopropyl triethoxysilane | Silane | KH550 | 2 |
| Polyether siloxane copolymer composition | Defoamer agent | – | 3 |
| Phenolic epoxy resin | Resin | – | 4 |
| Ethanol | Solvent | – | 3 |
| Ethylene glycol monobutyl ether | Solvent | – | 3 |
| <i>N</i> -methyl-2-pyrrolidone | Solvent | – | 3 |
| Diethanolamine | Modifier | – | 3 |
| Glacial acetic acid | Neutralization reagent | – | 3 |

Note: (1) Xilong Chemical Co. Ltd. (Guangzhou, China); (2) Qufu Chengguang Chemical Co. Ltd. (Jining, Shandong, China); (3) Tianjin Jinke Fine Chemical Institute (Tianjin, China); (4) Shandong Deyuan Epoxy Technological Co. Ltd. (Feicheng, Shandong, China).

2.2. Synthesis of Waterborne Coatings

PUA: The monomers of 24 g AA, 4 g ST, and 7 g EA with 44 g distilled water were blended in a three-neck glass reactor at 150 min^{-1} . Afterwards, the initiator (8g APS) was added at 10 wt %. In the next 70–90 min, the remaining 96 g AA, 16 g ST, and 133 g EA were dripped into the reactor. Afterwards, the remaining 32 g APS and 36 g KH550 were dripped into the reactor within 90–110 min. The reactor was heated up to $85 \text{ }^\circ\text{C}$ and kept for 4 h. The next step was to graft the pre-polyurethane onto the pre-polyarylate chain. For this step, 100 g TDI, 200 g PEG-400, and 8 g DBTD were dissolved in *N*-methyl-2-pyrrolidone solvent and blended into a three-neck glass reactor at 150 min^{-1} . The reactor was heated to $40 \text{ }^\circ\text{C}$. During stirring, 66 g HEA were dripped into the reactor within 2 h. The pre-polyurethane emulsion was obtained. Afterwards, both the pre-polyarylate and pre-polyurethane emulsions were mixed in the three-neck glass reactor and blended at 150 min^{-1} . The reactor was heated up to $85 \text{ }^\circ\text{C}$ and kept for 2 h. The PUA emulsion was obtained after cooling and filtration. A 2% defoamer agent was added into the emulsion at 100 min^{-1} for 10 min. The PUA waterborne coating was obtained with a solid content of 90 wt % and viscosity of $200 \text{ mPa}\cdot\text{s}$. It was kept in a black bottle and protected against light.

Epoxy resin: A 80 g portion of phenolic epoxy resin was added into a three-neck glass reactor at 150 min^{-1} . The reactor was heated up to $60 \text{ }^\circ\text{C}$ for 10 min. The solvent consisting of ethanol and ethylene glycol monobutyl ether was carefully poured into the reactor and stirred until the resin was completely dissolved. The reactor was then heated up to $80 \text{ }^\circ\text{C}$ and a 20 g portion of diethanolamine was dissolved in the ethanol (80 wt %) and dripped into the reactor within 1 h. The reaction was kept for 2 h. Then, the modified epoxy resin was obtained after removal of the solvent under vacuum. The modified epoxy resin was heated at $60 \text{ }^\circ\text{C}$ for 10 min and slowly dripped with glacial acetic acid for neutralization. The liquid was stirred for 30 min and the waterborne epoxy resin was obtained with a solid content of 90 wt % and viscosity of $150 \text{ mPa}\cdot\text{s}$. It was kept in a black bottle and protected against light.

2.3. Fabrication of Bamboo Scrimber

A bamboo column with a longitudinal dimensional of 2600 mm was split longitudinally into two semicircular tubes. The inner nodes were removed and then pushed into bamboo bundles with the removal of siliceous wax surfaces. Simultaneously, a series of dotted and linear cracks were formed on its surface. The diameter of the bamboo fiber bundle was lower than 0.2 mm. An impregnation process was employed to load phenol-formaldehyde (PF) resin. The target PF loading was 13 wt %. The bamboo bundles were immersed into the PF resin for 6 min at room temperature at a PF concentration of 22 wt %. Then, the bundles were taken out and laid aside for about 6 min to remove excess resin and weighed. The amount of resin was controlled by the solid content of resin and weight gains. The immersed bamboo bundle was dried in an oven at $70 \text{ }^\circ\text{C}$ to a constant weight, where the moisture content was about 12%. The fabrication of bamboo scrimber was carried out by a cold-in and cold-out process. The target density of the bamboo scrimber was 1.30 g/cm^3 . The bamboo bundles were assembled along the grain direction in a mold for hot-pressing. The pressure was kept at 3.5–7.0 MPa at $140 \text{ }^\circ\text{C}$ for 30 min for resin curing. Afterwards, cold water was introduced into the hot plate. When the temperature cooled down to $60 \text{ }^\circ\text{C}$, the pressure was released. The dimension of the bamboo scrimber was $2600 \times 1300 \times 16 \text{ mm}^3$. Subsequently, all mats were cut into the required dimensions and conditioned in a room at $20 \text{ }^\circ\text{C}$ and 65% RH for 2 weeks for further tests. The neat bamboo, which was designed as the control group, was prepared by the removal of inner and outer nodes of the bamboo tube, and cut into the dimensions of $2600 \times 35 \times 5 \text{ mm}^3$.

2.4. Coating

The Maso bamboo and BS were coated using a semi-automatic roll coater (BGD 218, BIUGED Laboratory Instruments, Guangzhou, China) according to ISO 15528:2000 [22] and the relative film thickness requirement. In theory, the dry film thickness was $18 \text{ }\mu\text{m}$. The film sample was then dried in a cool, dry, and dark environment for 1 week before use [23]. Three replicates were coated for each sample.

2.5. Film Physical Properties

The adhesion level, abrasion, and pencil hardness of the coating films were measured according to ISO 2409-2013 standard methods, the ISO 7784-2-2016 rubber wheel abrasion test, and the ISO 15184-2012 pencil hardness test [24–26], respectively. The adhesion test was carried out using a cross-cut knife, where the gap was about 2 mm. An adhesion tape was pasted on the center of the scratch and steadily peeled off. The detached coating along the intersections of the cuts was observed and the classification of 0–5 was made on the percentage of the detached area. The abrasion test was carried out using a Taber-type abrasion tester (TST-C1020, TST Instruments, Quanzhou, China) with a load of 500 g. P180-type abrasive papers were attached to the grinding wheel. The abrasion value was determined based on the weight loss after testing of 100 revolutions. The size of the testing sample was $100 \times 100 \text{ mm}^2$. For PUA- and epoxy resin-coated bamboo, three samples were spliced together by white latex in the direction of width to ensure a sufficient size. The pencil hardness test was carried out

on a car pencil hardness tester (QHQ-A, Tianjin Jinke Instrument, Tianjin, China), where a cylindrical hole was inclined at an angle of 45° for the pencil. A force of $7.5 \text{ kg}\cdot\text{m}\cdot\text{s}^{-2}$ for the tip of the pencil was applied on the surface of the sample. The results were determined by the lower level hardness of the pencil when defects occurred. To understand the inherent coating properties, the hardness and abrasion tests were performed on a non-permeable glass pane coated with the two types of coatings.

The thickness of the coating film was measured using a digital ultrasonic thickness gauge (PT700, Beijing Pengxiang Technological Co. Ltd., Beijing, China).

2.6. Characterizations of Basic Properties and Structures

The specimens, including coated and uncoated bamboo and coated and uncoated BS, were investigated. The chemical groups of the samples were examined using a Fourier transform infrared spectrometer equipped with an attenuated total reflection device (ATR-FTIR, BRUKER Vertex 70v, Hamburg, Germany). The specimens were put in contact with a ZnSe crystal at a 45° angle of incidence.

Samples of coated and uncoated bamboo and coated and uncoated BS with an area of $10 \times 10 \text{ mm}^2$ were prepared. The number of dominant functional groups present on the surface was characterized by X-ray photoelectron spectra (XPS) analysis (Escalab 250Xi, Thermo Scientific, Waltham, MA, USA). The pass energy was 10 eV and non-monochromatic $\text{MgK}\alpha$ and $\text{AlK}\alpha$ X-radiations ($h\nu = 1253.7$ and 1486.7 eV, respectively) was used with a current of 10 mA and a voltage of 13 kV. The survey scans were collected from the binding energy range of 0 to 1350 eV. The sample was mounted onto a holder with double-sided adhesive tape and vacuum-treated ranging from 1.33×10^{-6} to 1.33×10^{-5} Pa. The atomic percentages of the elements were obtained from the area of spectra.

The surface microstructures of the above samples were observed by SEM (JEOL JSM-6301F, Tokyo, Japan) with an acceleration voltage of 20 kV. Samples with an area of $10 \times 10 \text{ mm}^2$ were prepared and sputter-coated with gold using an ion sputter coater (ISC 150, SuPro Instruments, Shenzhen, China). The thickness of the gold was approximately 10 nm.

The surface morphologies were captured by atomic force microscopy (AFM) images, which were collected using a scanning probe microscope (Dimension Fast Scan, Bruker, Hong Kong, China) in contact mode. The tested area was $2 \times 2 \mu\text{m}^2$. For each sample, three replicates were carried out.

3. Results and Discussion

3.1. Chemical Synthesis and Curing Process

According to relevant studies [15–20], the chemical synthesis processes of the two kinds of coatings are shown in Figure 1. As seen in Figure 1a, first, the addition action occurred in the C=C bonds of the AA, ST, and EA in the case of initiator. Thereafter, the silane KH550 grafted onto the main chains and the pre-polyarylate was synthesized. In the third step, the polycondensation reaction occurred between the O=C=N groups of TDI and the –OH groups of PEG-400. Simultaneously, the HEA grafted onto the main chains at the end group of O=C=N, and the pre-polyurethane was synthesized. Finally, the pre-polyarylate and pre-polyurethane bonded together via C=C bond addition action. As for the epoxy resin (Figure 1b), part of the epoxy groups reacted with the N–H group of diethanolamine, which turned the hydrophobic resin into hydrophilicity and soluble in water. Finally, the modified resin was neutralized by glacial acetic acid.

The curing process of the water-based coatings on wood substrates can be divided into three steps. First, the water slowly evaporated, and the small particles of the coating moved closer to each other. Second, the water kept on evaporating and the small particles squeezed, forming a continuous film. Third, with the final evaporation of residue water, some of the small particles penetrated into the wooden substrates through capillary force, and others squeezed with each other, forming a smooth film layer.

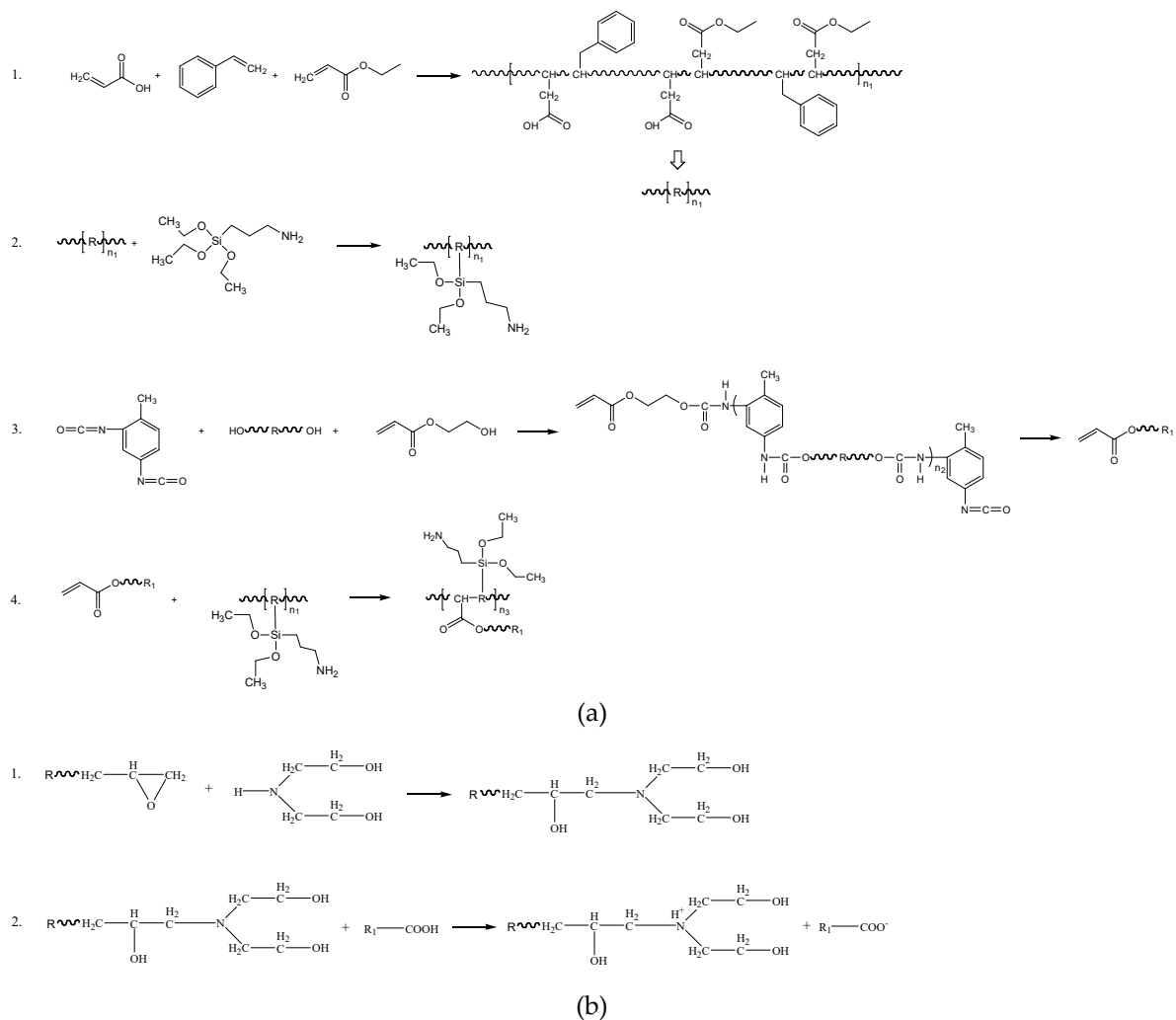


Figure 1. Chemical synthesis processes of the two kinds of coatings. (a) Polyurethane acrylate (PUA); (b) epoxy resin.

3.2. Chemical Analysis

The ATR-FTIR results of the specimens, including coated and uncoated bamboo, and the BS are shown in Figure 2. Figure 2a shows the results of the uncoated specimens. From Figure 2a, chemical group bands in intensity varied between the two specimens, which indicated that there were chemical reactions during the preparation of the bamboo scrimber [11]. The absorption band of $\text{C}=\text{O}$ at 1737cm^{-1} is the characteristic band of hemicellulose. In the case of the BS, this band almost disappeared, which indicated that the hemicellulose and polysaccharide of bamboo degraded during curing. The absorption band at 1475cm^{-1} is the characteristic band of the $-\text{CH}_2$ and the band of BS significantly increased, which indicated that much phenolic resin was added to the bamboo materials. In addition, the $\text{C}-\text{O}$ absorption band of BS at 1043cm^{-1} increased, and the $\text{C}-\text{O}$ vibration band of the ester bond at 1265cm^{-1} shifted to 1240cm^{-1} , which indicated that aromatic ester bonds and ether bonds formed between the phenolic resin and cellulose. The skeletal stretching vibration band of the lignin aromatic benzene ring $\text{C}=\text{C}$ at 1630cm^{-1} of BS shifted to 1607cm^{-1} , which was due to the side chain substitution on the lignin benzene ring during heating [27,28].

Figure 2b shows the ATR-FTIR results of the specimens coated with PUA. There was little difference in the ATR-FTIR between coated bamboo and coated BS, which indicated that the coating covered the surface of materials and formed a paint film. In addition, the characteristic absorption bands attributed to the polyurethane acrylate coating were reflected in the spectrum, including

3414 cm^{-1} ($-\text{OH}$ stretching vibration), 2940 cm^{-1} ($-\text{CH}_2/\text{CH}_3$ symmetry and antisymmetric stretching vibration), 1736 cm^{-1} $\text{C}=\text{O}$ of ester stretching vibration), 1671 cm^{-1} ($\text{C}=\text{O}$ in unsaturated acid stretching vibration), 1549 cm^{-1} ($-\text{NH}_2$ stretching vibration), 1485 cm^{-1} ($-\text{CH}_2$ in-plane bending vibration), 1383 cm^{-1} ($-\text{OH}$ in-plane bending vibration), 1248 cm^{-1} ($\text{C}-\text{O}$ of ester stretching vibration), 1080 cm^{-1} ($\text{C}-\text{O}$ of ether stretching vibration), 1010 cm^{-1} ($\text{C}-\text{OH}$ stretching vibration), 910 cm^{-1} ($-\text{OH}$ of acid out-of-plane bending vibration), 812 cm^{-1} ($-\text{NH}$ out-of-plane bending vibration), and 620 cm^{-1} ($-\text{CH}_2$ out-of-plane bending vibration) [28,29].

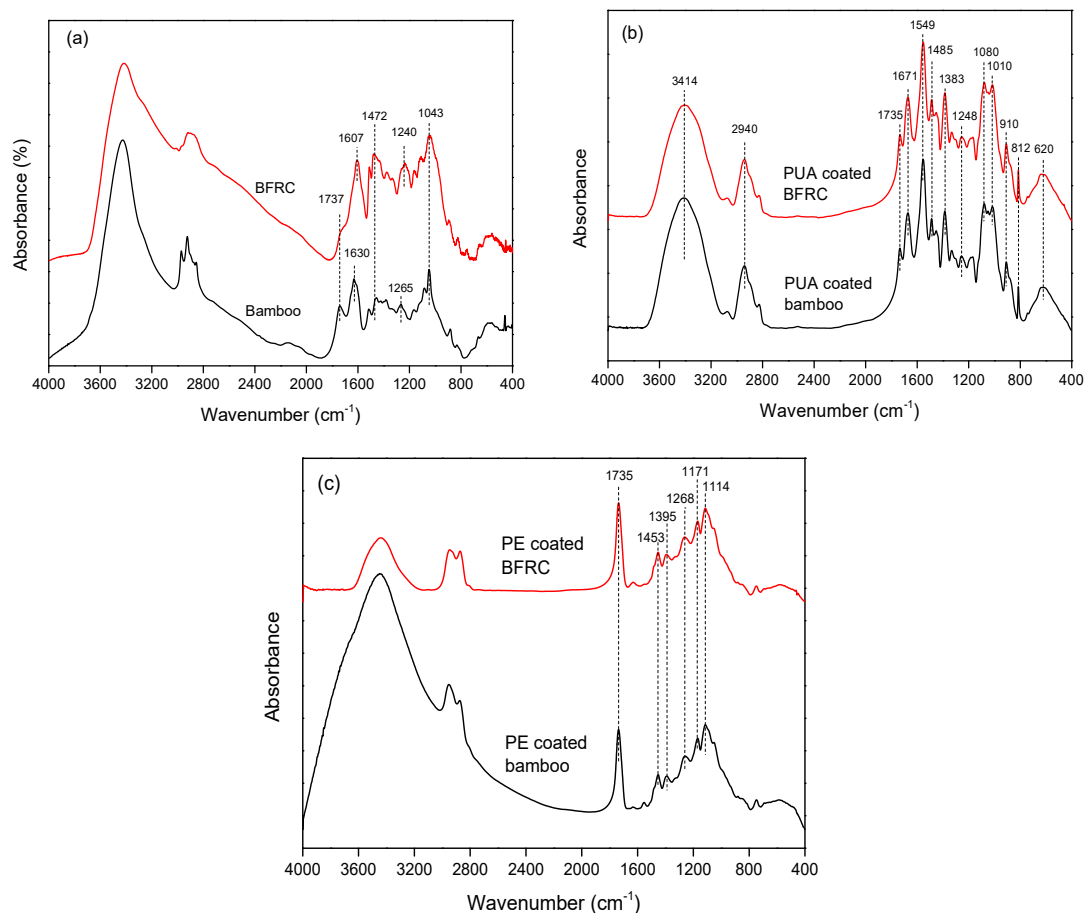


Figure 2. ATR-FTIR of (a) uncoated bamboo/BS and (b) bamboo/BS coated with PUA and (c) epoxy resin.

Figure 2c shows the ATR-FTIR results of the specimens coated with the epoxy resin. Unlike the specimens coated with polyurethane acrylate, there were some differences between coated bamboo and coated BS in the range of 4000 to 2800 cm^{-1} . Among them, the symmetry and antisymmetric stretching vibration of $-\text{CH}_2$ at 2950 and 2870 cm^{-1} of bamboo coated with epoxy resin was weak. In the range of 2000 to 400 cm^{-1} , the spectrum of coated bamboo was basically the same as the spectrum of coated BS, where both exhibited the characteristic of the epoxy resin coating, including 1735 cm^{-1} ($\text{C}=\text{O}$ stretching vibration in the fatty amine curing agent), 1453 cm^{-1} ($-\text{CH}_2$ in-plane bending vibration), 1395 cm^{-1} ($-\text{CH}$ in-plane bending vibration), 1268 cm^{-1} ($\text{C}=\text{O}$ stretching vibration of ester bond), 1171 cm^{-1} (alkane skeleton $\text{C}-\text{C}$ stretching vibration), and 1114 cm^{-1} ($-\text{C}-\text{OH}$ stretching vibration) [28,30].

Table 2 shows the percentage results of XPS elements of each sample before and after coating. The atomic percentages of C, O, and N in bamboo were 70.35%, 26.63%, and 3.02%, respectively. After fabricating the bamboo into BS, the element C increased to 78.37%, whereas the element O decreased and the N content was essential unchanged. The reason may be associated with the higher content of C in PF resin, which was added into the BS. For the bamboo coated with PUA, the atomic percentages

of C, O, and N were 74.77%, 20.43%, and 4.81%, respectively. Compared with uncoated bamboo, the contents of C and N increased, and the content of O decreased, which was due to the presence of more C and N elements in the PUA coating. In addition, the C of the BS, coated with PUA, was basically the same as the coated bamboo, but the N content was significantly increased. The explanation is that the PF resin in the reconstituted bamboo could react with the ester groups of the urethane acrylate. Thus, more amino groups were exposed on the surface of the sample and more N was obtained. Another possible reason may be associated with the film thickness. The BS coated with PUA showed a larger film thickness than the bamboo coated with PUA, indicating the difficulty for PUA penetrating into the BS. Therefore, the N content was higher. The C element of bamboo, coated with epoxy resin, was significantly increased to 81.10%, and the O element greatly decreased, which was due to the epoxy coating that coated the substrate surface. However, the C content of BS, coated with the epoxy coating, was lower than that of the coated bamboo, which indicated that the epoxy group was more likely to react with the hydroxyl group of bamboo and the O content decreased [31]. In addition, the larger film thickness of the epoxy resin-coated BS contributed to the larger O content.

Table 2. Element contents of uncoated and coated bamboo/BS by XPS analysis.

| Samples | Element Content (%) | | |
|--------------------------------------|---------------------|-------|------|
| | C | O | N |
| Bamboo | 70.35 | 26.63 | 3.02 |
| BS | 78.37 | 19.01 | 2.62 |
| Bamboo coated with PUA | 74.77 | 20.43 | 4.81 |
| BS coated with PUA | 74.21 | 17.61 | 8.18 |
| Bamboo coated with the epoxy coating | 81.19 | 17.06 | 1.75 |
| BS coated with the epoxy coating | 78.56 | 19.86 | 1.58 |

In order to further analyze the binding of C in each material, the four bands were observed, including C1 (C–C/C–H), C2 (C–O/C–OH), C3 (O–C–O/C=O), and C4 (O–C=O) [32]. The results are shown in Figure 3 and Table 3. It can be seen that there is no C4 band except for the BS sample coated with PUA. It may be due to the fact that PUA contains ester bonds and has poor permeability with respect to recombinant bamboo, resulting in a large accumulation of PUA molecules, thus detecting a small amount of C4 bands. The proportions of C1, C2, and C3 in bamboo were 54.82%, 34.78%, and 10.40%, respectively. In contrast, the proportion of C1 of BS increased significantly, and the proportion of C2 decreased, due to the PF resin containing a large amount of C–H. Moreover, there was no C3 band in the samples coated with the epoxy coating, which indicated that there were few ketones and aldehydes in the epoxy coating. In addition, a higher C1 content and a lower C2 content were observed in the coated bamboo as compared with those in the coated BS. This was mainly because the epoxy bond of the coating reacted with the –OH on the bamboo/BS surface so that less residual C–OH was present.

Table 3. C element contents of uncoated and coated bamboo/BS by XPS analysis.

| Samples | Element Content (%) | | | |
|--------------------------------------|---------------------|-------|-------|------|
| | C1 | C2 | C3 | C4 |
| Bamboo | 54.82 | 34.78 | 10.40 | 0 |
| BS | 72.51 | 19.35 | 8.14 | 0 |
| Bamboo coated with PUA | 68.81 | 18.96 | 12.23 | 0 |
| BS coated with PUA | 66.09 | 22.42 | 7.58 | 3.91 |
| Bamboo coated with the epoxy coating | 75.10 | 20.39 | 0 | 4.51 |
| BS coated with the epoxy coating | 69.35 | 25.23 | 0 | 5.43 |

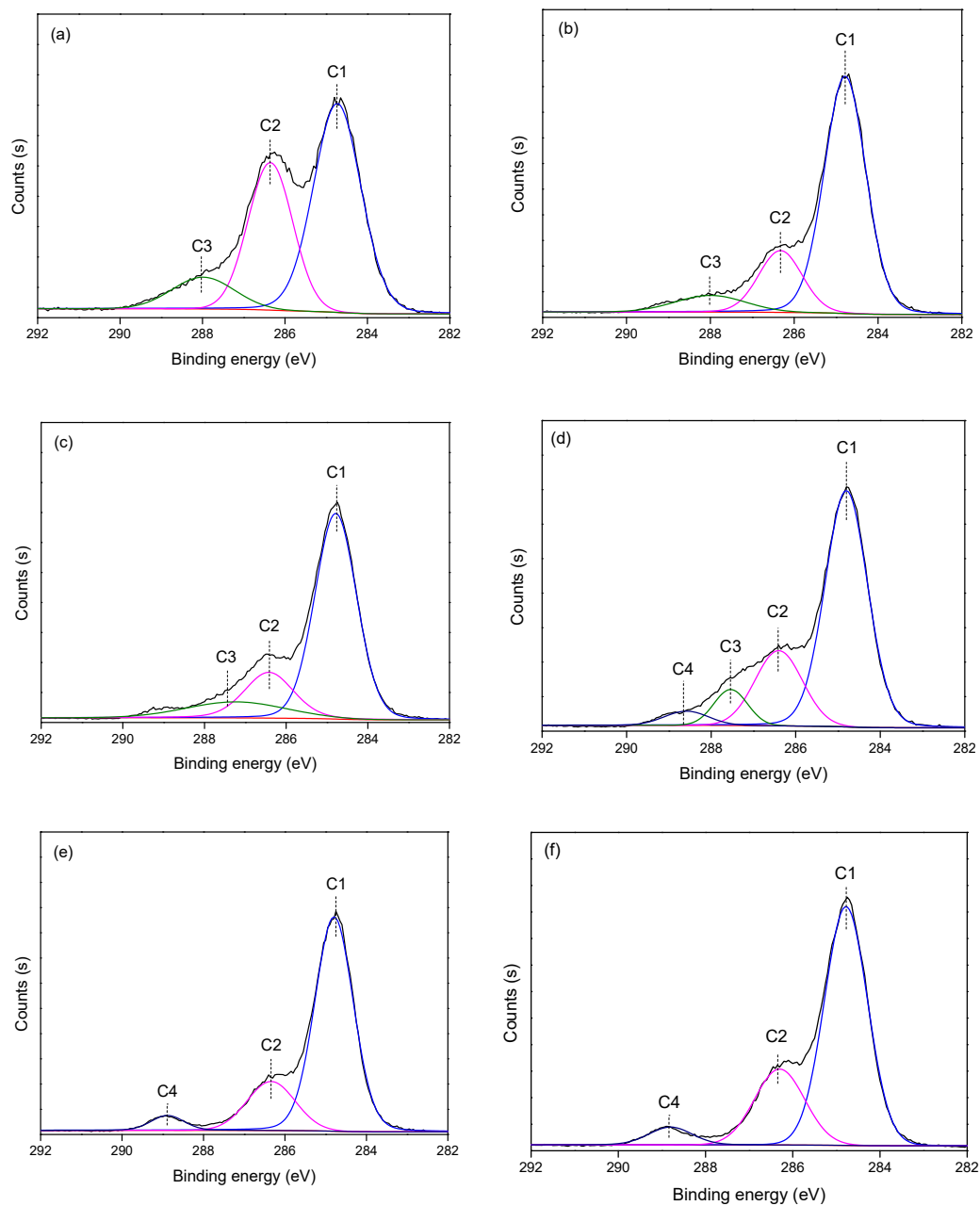


Figure 3. XPS C-band spectra of bamboo, BS, and coated samples: (a) bamboo; (b) BS; (c) bamboo coated with PUA; (d) BS coated with PUA; (e) bamboo coated with the epoxy coating; (f) BS coated with the epoxy coating.

3.3. Morphologies

The surface morphologies of each sample before and after coating are shown in Figure 4. The microstructure of the bamboo was clearly observed before coating, including the dense bamboo fibers and looser parenchyma cells. After the recombinant processing into BS, the parenchyma cells of bamboo were destroyed and the cell structure became dense. When coated with PUA, the sample surface was well covered. Therefore, a flat coating film was received. There was a small number of micro-nano-particle protrusions on the surface of the PUA coating samples. It may be due to the bubbling caused by the penetration of the coating into the interior of the BS during the curing process. The result was as same as the XPS results and could be also inferred from the film thickness results. On the other hand, for the samples coated with epoxy, the particles and bubbles on the surface

were obviously increased, indicating that the epoxy coating had a better permeability with respect to bamboo, but its covering ability was poor and an uneven coating film was obtained. In addition, the epoxy coating was more likely to agglomerate on the surface of the BS, so that more bubbles on the surface of the BS were observed [33].

AFM can show the morphology of coating and obtain the roughness of the sample at nanometer scale [34]. The surface topography of the coated samples is shown in Figure 5. The roughness obtained by AFM is listed in Table 4. As can be seen from the figure, bamboo and BS were both well covered by PUA and a smooth film surface was obtained, with few defects in the small area that was assessed. Tiny flow marks of the coating film could be seen on the surface of the bamboo, with a surface roughness value of 1.35 nm. The coating film surface of BS was rougher after drying, with an average roughness value of only 1.41 nm. Compared with the samples coated with PUA, the surface roughness of the samples coated with epoxy was greater, which was consistent with the SEM results. The surface defects of the samples coated with epoxy were significant, and the maximum roughness value was 2.79 nm.

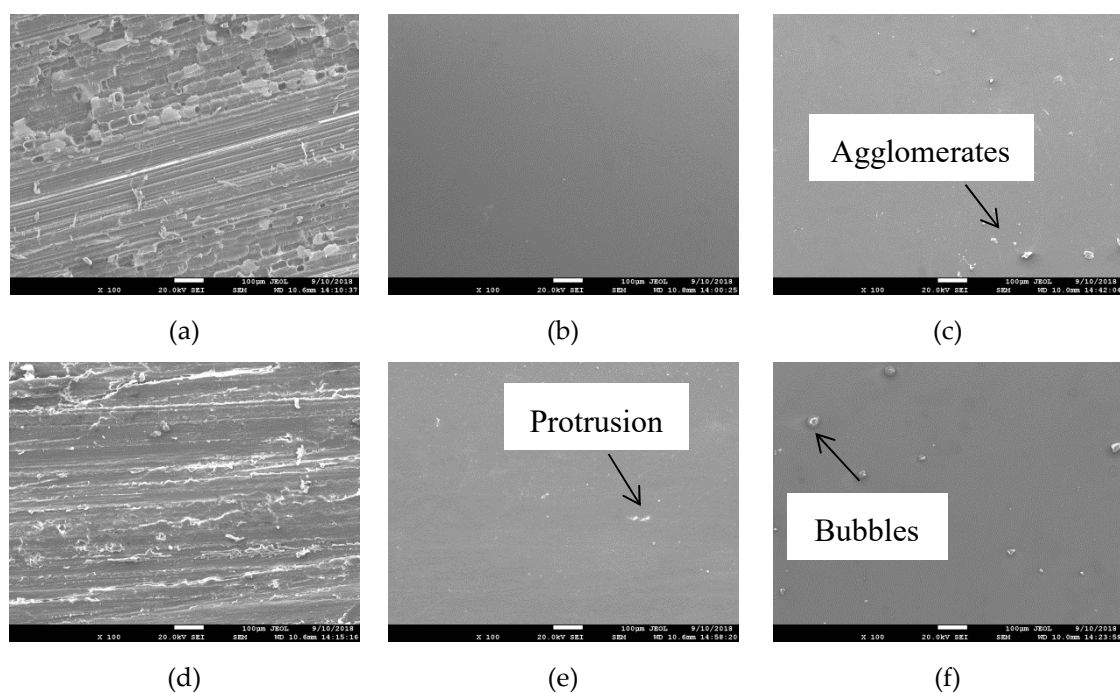


Figure 4. SEM of uncoated and coated bamboo/BS: (a) bamboo; (b) bamboo coated with PUA; (c) bamboo coated with epoxy resin; (d) BS; (e) BS coated with PUA; (f) BS coated with epoxy resin.

Table 4. Adhesion level, hardness, abrasion value, film thickness, and roughness of coating films of coated bamboo and BS.

| Samples | Adhesion Level | Hardness | Abrasion Value (g/100r) | Dry Film Thickness (μm) | Roughness (nm) |
|--|----------------|----------|-------------------------|--------------------------------------|----------------|
| Glass pane coated with PUA | – | 4H | 0.168 | – | 0.65 |
| Bamboo coated with PUA | 2 | H | 0.088 | 10.6 | 1.35 |
| BS coated with PUA | 2 | H | 0.092 | 13.9 | 1.41 |
| Glass pane coated with the epoxy coating | – | 2H | 0.188 | – | 0.72 |
| Bamboo coated with the epoxy coating | 1 | HB | 0.075 | 8.7 | 1.89 |
| BS coated with the epoxy coating | 2 | HB | 0.122 | 15.4 | 2.79 |

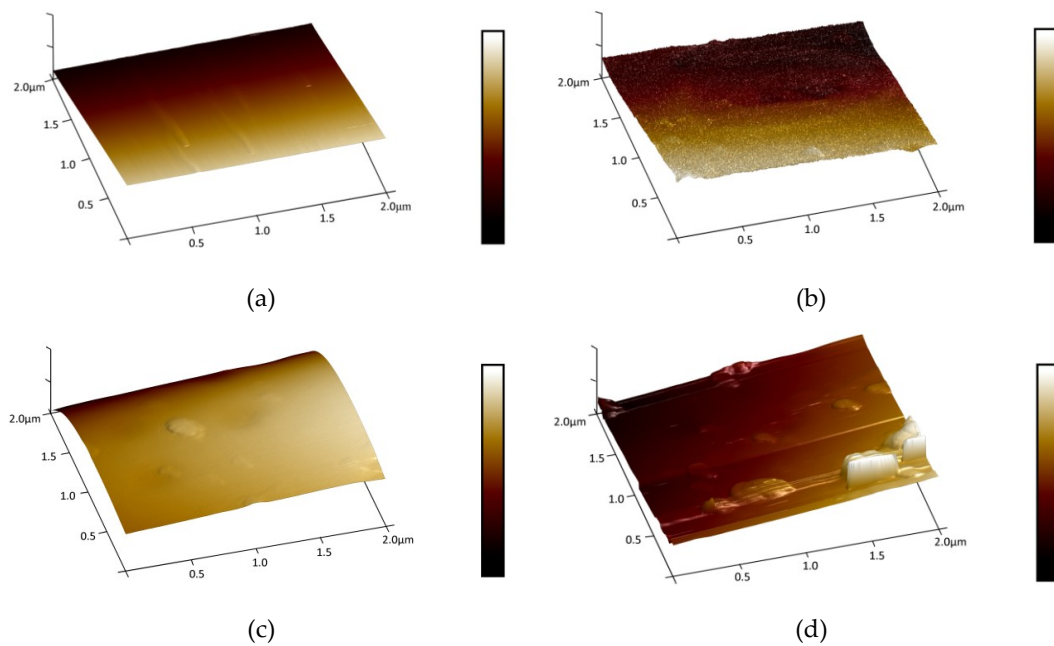


Figure 5. AFM of coated bamboo/BS: (a) bamboo coated with PUA; (b) BS coated with PUA; (c) bamboo coated with epoxy resin; (d) BS coated with epoxy resin.

3.4. Surface Properties

The adhesion of coating films for coated bamboo and coated BS is shown in Figure 6. It can be seen from the figure that in addition to the coating film adhesion of the epoxy-coated bamboo of 1 level, the coating film adhesion of the other samples were all 2 level, which was probably because epoxy resin could penetrate into bamboo well compared with PUA, but the permeability with respect to BS was poor.

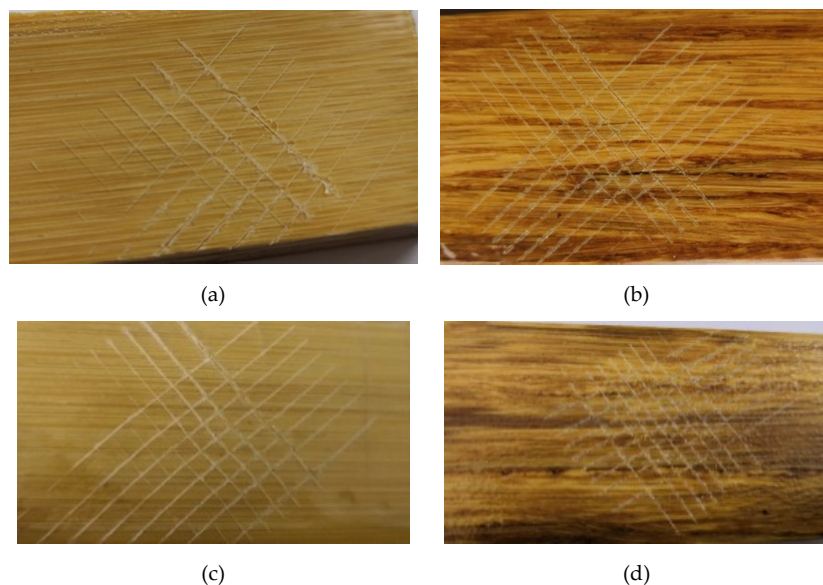


Figure 6. The adhesion images of coating films of coated bamboo and BS: (a) bamboo coated with PUA; (b) BS coated with PUA; (c) bamboo coated with epoxy resin; (d) BS coated with epoxy resin.

The adhesion level, hardness, abrasion value, film thickness, and roughness of coating films of coated bamboo and coated BS are shown in Table 4. From the results, we can see that the hardness and abrasion resistance of PUA was higher than that of epoxy coating (see the results on the glass

pane). However, when the substrates changed to bamboo and BS, the results were different. It seemed that the hardness decreased while the abrasion resistance was improved due to the permeability of coatings with respect to the bamboo and BS. Compared with the effects of two types of coatings, the tendency was almost the same. The coating film hardness of the bamboo and BS coated with PUA was H, which was higher than the HB hardness of the samples coated with epoxy. The bamboo coated with epoxy had the highest coating film adhesion and the lowest abrasion value of 0.075 g/100r, and the lowest film thickness value of 8.7 μm . However, the abrasion value of BS coated with the epoxy coating was the highest, which may be associated with the high film thickness, roughness, and also the inherent property of the coatings. As mentioned, the SEM analysis showed that more bubbles were found on the surface of the BS coated with the epoxy coating. Thus, its surface performance was poor.

4. Conclusions

In the case of different coatings and substrates, the coating performance varied. Compared with bamboo, BS had a poorer performance, whether the coating was PUA or epoxy. On the other hand, different coatings had different finishing coating properties for bamboo scrimber with the better adhesion level and hardness and the low abrasion value. However, the PUA-coated samples had smoother surfaces with an adhesion level of 2 and a pencil hardness of H. Moreover, the abrasion value of PUA-coated samples was acceptable in the range of 0.088–0.092 g/100r. Further study on the coating mechanism of different waterborne coatings on bamboo scrimber should be done as the next step, and a new kind of waterborne coating should be developed to further improve coating performance.

Author Contributions: Writing—Original Draft Preparation, J.X.; Investigation, R.L.; Data Curation, H.W.; Software, H.Q.; Methodology, Y.Y.; Conceptualization, L.L.; Writing—Review and Editing, Y.N.

Funding: This study was funded by the National Natural Science Foundation of China (Nos. 31870550, 31470591) and the National Key Research and Development Program of China (No. 2016YFD0600704).

Conflicts of Interest: The authors declare no conflict of interest.

References

- Xie, Y.; Xie, G.; Yao, Q. Present situation and outlook of bamboo resource utilization in China. *Chin. J. Trop. Agric.* **2004**, *6*, 46–52.
- Yu, Y.; Huang, X.; Yu, W. A novel process to improve yield and mechanical performance of bamboo fiber reinforced composite via mechanical treatments. *Compos. Part B Eng.* **2014**, *56*, 48–53. [[CrossRef](#)]
- Mahdavi, M.; Clouston, P.L.; Arwade, S.R. A low-technology approach toward fabrication of laminated bamboo lumber. *Constr. Build. Mater.* **2012**, *29*, 257–262. [[CrossRef](#)]
- Shangguan, W.; Zhong, Y.; Xing, X.; Zhao, R.; Ren, H. 2D model of strength parameters for bamboo scrimber. *BioResources* **2014**, *9*, 7073–7085. [[CrossRef](#)]
- Shangguan, W.; Gong, Y.; Zhao, R.; Ren, H. Effects of heat treatment on the properties of bamboo scrimber. *J. Wood Sci.* **2016**, *62*, 383–391. [[CrossRef](#)]
- Sharma, B.; Gatóo, A.; Bock, M.; Ramage, M. Engineered bamboo for structural applications. *Constr. Build. Mater.* **2015**, *81*, 66–73. [[CrossRef](#)]
- Meng, F.; Yu, Y.; Zhang, Y.; Yu, W.; Gao, J. Surface chemical composition analysis of heat-treated bamboo. *Appl. Surf. Sci.* **2016**, *371*, 383–390. [[CrossRef](#)]
- Yu, Y.; Liu, R.; Huang, Y.; Meng, F.; Yu, W. Preparation, physical, mechanical, and interfacial morphological properties of engineered bamboo scrimber. *Constr. Build. Mater.* **2017**, *157*, 1032–1039. [[CrossRef](#)]
- Wei, Y.; Ji, X.; Duan, M.; Li, G. Flexural performance of bamboo scrimber beams strengthened with fiber-reinforced polymer. *Constr. Build. Mater.* **2017**, *142*, 66–82. [[CrossRef](#)]
- Zhong, Y.; Wu, G.; Ren, H.; Jiang, Z. Bending properties evaluation of newly designed reinforced bamboo scrimber composite beams. *Constr. Build. Mater.* **2017**, *143*, 61–70. [[CrossRef](#)]
- Meng, F.; Liu, R.; Zhang, Y.; Huang, Y.; Yu, Y.; Yu, W. Improvement of the water repellency, dimensional stability, and biological resistance of bamboo-based fiber reinforced composites. *Polym. Compos.* **2019**, *40*, 506–513. [[CrossRef](#)]

12. Amada, S.; Ichikawa, Y.; Munekata, T.; Nagase, Y.; Shimizu, H. Fiber texture and mechanical graded structure of bamboo. *Compos. Part B Eng.* **1997**, *28*, 13–20. [[CrossRef](#)]
13. Sulastingsih, I.M.; Nurwati. Physical and mechanical properties of laminated bamboo board. *J. Trop. For. Sci.* **2009**, *3*, 246–251.
14. Kumar, A.; Vlach, T.; Laiblova, L.; Hroudá, M.; Kasal, B.; Tywoniak, J.; Hajek, P. Engineered bamboo scrimber: Influence of density on the mechanical and water absorption properties. *Constr. Build. Mater.* **2016**, *127*, 815–827. [[CrossRef](#)]
15. Liptáková, E.; Kúdela, J.; Sarva, J. Study of the system wood-coating material. I. wood-liquid coating material. *Holzforschung* **2000**, *2*, 189–196. [[CrossRef](#)]
16. Schaller, C.; Rogez, D. New approaches in wood coating stabilization. *J. Coat. Technol. Res.* **2007**, *4*, 401–409. [[CrossRef](#)]
17. Long, L.; Xu, J.; Wan, X. Surface modification of nano-alumina and its application in preparing polyacrylate water-based wood coating. *J. Polym. Eng.* **2013**, *33*, 767–774. [[CrossRef](#)]
18. Liptáková, E.; Kúdela, J. Study of the system wood-coating material. Part 2. Wood-solid coating material. *Holzforschung* **2002**, *5*, 547–557. [[CrossRef](#)]
19. Queant, C.; Blanchet, P.; Landry, V.; Schorr, D. Effect of adding UV absorbers embedded in carbonate calcium templates covered with light responsive polymer into a clear wood coating. *Coatings* **2018**, *8*, 265. [[CrossRef](#)]
20. Frigione, M.; Lettieri, M. Novel attribute of organic–inorganic hybrid coatings for protection and preservation of materials (stone and wood) belonging to cultural heritage. *Coatings* **2018**, *8*, 319. [[CrossRef](#)]
21. Li, C.; Xiao, H.; Wang, X.; Zhao, T. Development of green waterborne UV-curable vegetable oil-based urethane acrylate pigment prints adhesive: Preparation and application. *J. Clean. Prod.* **2018**, *180*, 272–279. [[CrossRef](#)]
22. *ISO 15528:2000 Paints, Varnishes and Raw Materials for Paints and Varnishes-Sampling*; ISO: Geneva, Switzerland, 2000.
23. Xu, J.; Wu, H.; Liu, R. Preparation and properties of light-resistant UV ink modified with nano-TiO₂ on wood substrate. *Surf. Eng.* **2018**. [[CrossRef](#)]
24. *ISO 2409-2013 Paints and Varnishes-Cross-Cut Test*; ISO: Geneva, Switzerland, 2013.
25. *ISO 7784-2-2016 Paints and Varnishes—Determination of Resistance to Abrasion—Part 2: Method With Abrasive Rubber Wheels and Rotating Test Specimen*; ISO: Geneva, Switzerland, 2016.
26. *ISO 15184-2012 Paints and Varnishes—Determination of Film Hardness by Pencil Test*; ISO: Geneva, Switzerland, 2012.
27. Mandla, A.T.; Peter, K.; Mark, R.V. Surface chemistry and moisture sorption properties of wood coated with multifunctional alkoxy silanes by sol-gel process. *J. Appl. Polym. Sci.* **2003**, *88*, 2828–2841.
28. Ray, A.K.; Das, S.K.; Mondal, S.; Ramachandrarao, P. Microstructural characterization of bamboo. *J. Mater. Sci.* **2004**, *39*, 1055–1060. [[CrossRef](#)]
29. Sun, R.H.; Li, X.J.; Hou, R.G.; Qiao, J.Z. Effects of high temperature heat treatment on FTIR and XRD characteristics of bamboo bundles. *J. Cent. Sout. Fore. Tech.* **2013**, *2*, 97–100.
30. Rao, J.; Bao, L.; Wang, B.; Fan, M.; Feo, L. Plasma surface modification and bonding enhancement for bamboo composites. *Compos. Part B Eng.* **2018**, *138*, 157–167. [[CrossRef](#)]
31. Kocaefe, D.; Huang, X.; Kocaefe, Y.; Boluk, Y. Quantitative characterization of chemical degradation of heat-treated wood surfaces during artificial weathering using XPS. *Surf. Interface Analy.* **2013**, *45*, 639–649. [[CrossRef](#)]
32. Gironès, J.; Méndez, J.A.; Boufi, S.; Vilaseca, F.; Mutjé, P. Effect of silane coupling agents on the properties of pine fibers/polypropylene composites. *J. Appl. Polym. Sci.* **2007**, *103*, 3706–3717. [[CrossRef](#)]
33. Zou, L.; Jin, H.; Lu, W.Y.; Li, X. Nanoscale structural and mechanical characterization of the cell wall of bamboo fibers. *Mater. Sci. Eng. C* **2008**, *29*, 1375–1379. [[CrossRef](#)]
34. Meincken, M.; Evans, P.D. Nanoscale characterization of wood photodegradation using atomic force microscopy. *Eur. J. Wood Prod.* **2009**, *67*, 229–231. [[CrossRef](#)]

